Relating soil organic matter composition to soil water repellency for soil biopore surfaces different in history from two Bt horizons of a Haplic Luvisol

Haas, C.[1]*, Gerke, H.H. [2], Ellerbrock, R.H. [2], Hallett, P.D. [3], Horn, R. [1]

*corresponding author: c.haas@soils.uni-kiel.de

[1]Institute for Plant Nutrition and Soil Science, CAU Kiel, Hermann-Rodewald-Str. 2, 24118 Kiel, Germany

[2]Institute of Soil Landscape Research, Leibnitz Centre for Agricultural Landscape Research, Eberswalder Str. 84, 15374 Müncheberg, Germany

[3] School of Biological Sciences, University of Aberdeen, Aberdeen AB24 3UU, UK

Relating soil organic matter composition to soil water repellency

Abstract

The deposition of organic matter (OM), which is known for its high potential water repellency, on biopore walls can enhance preferential flow through these pores. In this study OM composition determined with DRIFT spectroscopy was related to soil water repellency (SWR) determined with Sessile Drop method (SDM), Wilhelmy-plate method (WPM), and sorptivity tests. We hypothesized that the chemical composition (in terms of PWI) is (i) related to the physical properties (i.e., contact angle) of biopore walls, (ii) depends on the history of the biopore and (iii) differs from the bulk soil matrix. Thus, the main objective was to identify the relation between OM composition determined with DRIFT spectroscopy and SWR in structured soils. The experiments were carried out on biopores and their surrounding soil matrices, excavated from two depths of a haplic Luvisol, with three different biopore histories (i.e., root channels, earthworm burrows, and root channels which were short-term colonized by an earthworm). All measurements at intact biopore surfaces indicated a

larger SWR at the surface of biopore walls as compared to the surrounding matrices, and showed a higher proportion of hydrophobic functional groups. The OM composition determined with DRIFT spectroscopy correlated ($R^2 > 0.7$) with contact angles (SDM-method) which is in line with results of both water sorptivity and WPM for soils with reduced wettability. The surfaces of short-term colonized earthworm burrows had the most varying hydrophobic to hydrophilic components (A/B)-ratio of all investigated biopore surfaces depending on soil depth. For biopore surfaces at this depth contact angles >90° were frequently observed. The results also indicate that earthworms can lower SWR by aggregate disruption.

1. Introduction

Preferential flow paths like earthworm burrows and root channels (Jarvis, 2007) play a major role for gas, water, and heat fluxes in soils. Beside these indirect influences of macropores on the fertility of structured soils, biopores may act as pathways for roots to propagate into deeper soil layers where water and nutrient uptake can be enhanced (Kautz et al., 2012). Organic matter (OM) is known for coating the outermost layer of mineral particles (Doerr et al., 2000; Ellerbrock and Gerke, 2004).

Elluvial processes, which (especially) occur in Luvisols (Ap/E/Bt/C horizon sequence), are characterized by leaching dissolved organic substances (DOC) and clay particles from the A-and E-horizon to the B horizon, respectively, resulting in clay (-organo-)coatings at the surfaces of soil aggregates. On the other hand, earthworms and roots exude numerous mostly organic compounds like sugars, amino acids and terpenes but also carbon dioxide (Scheu, 1991; Jones et al., 2009). The total amount and composition of the exudates varies with organism age, species, feeding, health status and soil environmental conditions (Carvalhais et al., 2010; Christiansen-Weniger et al., 1992; Jones 2009). There is also scope to modify organic compounds released to biopore surfaces through plant breeding, as large differences between crop cultivars have been observed (Christiansen-Weniger et al., 1992). Furthermore, decayed plant roots (debris, fine root hairs) increase the carbon content in the rhizosphere (for a review see Six et al., 2004). All these processes result in altered soil properties compared to the bulk soil (Nunan et al., 2003). In consequence bioturbation by earthworms or roots can cause biopores with concentrated OM along their walls (Kautz et al., 2012). Both, the outermost layer of soil aggregates, as well

as the surface of biopores are hot-spots in terms of microbial activity (Kuzyakov & Blagodatskaya, 2015; Hoang et al., 2016), and interaction between percolating water, reactive solutes and the soil matrix.

Aggregation next to biopores is influenced by two factors, both enhancing soil aggregation: (i) organic compounds, sometimes coupled with the presence of decaying roots may stick together mineral particles (Six et al., 2006) and (ii) plants may enhance wetting and drying (Vetterlein and Marschner, 1993) and coincide shrinkage and swelling (Horn et al., 1994; Peng and Horn, 2005). Beside other influences, aggregate development is also affected by the pH, since protons can act as a monovalent cation. While the soil around roots can become more acidic (Uteau et al., 2015) due to the roots' release of CO_2 and H^+, the soil around earthworm burrows can be more neutral/alkaline caused by the earthworms' release of $CaCO_3$ from specialized oesophageal glands which were discovered by Lankester (1865). Some earthworms are also able to affect the pH in their environment (Sizmur et al., 2011). However, bioturbation can also homogenize soil aggregates, e.g. at high water contents (Horn et al., 1994), forming an unstructured mixture that release stabilized organic matter (Six et al., 2006) and an intermixture of aggregate surfaces with their interiors (Bossuyt et al., 2005). Such processes often result in heterogeneous distributions and compositions of organic matter at a small scale that in turn may influence soil properties like contact angle.

The wettability of intact biopore surfaces created by either earthworms or plant roots has been intensively studied (e.g., Leue et al., 2010b, 2013, 2016; Urbanek et al., 2014). It is often related to the soil organic carbon content (Urbanek et al., 2014; Zheng et al., 2016). But organic matter in soil (SOM) is a heterogeneous mixture of organic components containing hydrophilic (C=O) and hydrophobic (C-H) functional groups that can be determined with infrared spectroscopy (e.g., Ellerbrock and Gerke, 2004). The ratio between the C-H absorption band intensities (i.e., a measure for hydrophobic groups) and the C=O absorption band intensities (i.e., a measure for hydrophilic groups), the C-H/C=O-ratio, was found to be related to the wettability of soil samples (e.g., Ellerbrock et al., 2005) and was defined as a potential wettability index (PWI; Leue et al., 2013). However, there is a lack in information about alteration in surface properties of both, earthworm burrows and plant root channels induced by earthworm activity.

Beside the PWI, a couple of methods for the assessment of the wettability of soils are available (Bachmann et al., 2003). While contact angles can be measured directly with the sessile drop method, indirect measurements such as sorptivity tests or capillary rise method (contact angle derived by comparing for example flow-rates of ethanol with that of water) or the time that droplet of an ethanol-water mixture of a certain molality need to penetrate (Bachmann et al., 2003; Moody and Schlossberg, 2010) represent the methods used in general. But there is a lack in relating spectral information on the PWI of SOM composition at intact surfaces with their wettability properties.

Our aim was to investigate the influence of earthworms, plant roots, and their effects on the potential wettability index (PWI). Two experimental setups were used to measure the PWI on different scales. And we linked the PWI with a physical property: contact angles determined from sessile drop method, sorptivity tests and the Wilhelmy plate method.

We hypothesized that the chemical composition (in terms of PWI) is (i) related to the physical properties (i.e., contact angle) of biopore walls, (ii) depends on the history of the biopore and (iii) differs from the bulk soil matrix. Furthermore, we expected that the chemical composition of organic compartments is distributed more heterogeneously if measured on a smaller scale. We expected an increasing degree of scattering with increasing spatial resolution, reflecting the small-scaled heterogeneity of intact biopore walls or, more generally, of soils. With a view to soil ecology and e.g., hydraulic processes, a smaller-scaled analysis seemed useful, because biopore walls may contain large numbers of pinholes that can act as a preferential flow path from the biopore surface into the surrounding matrix. The quality of the organic matter of these pinholes can differ from those of biopore walls (Leue et al., 2016). Since these very small pinholes can have a huge hydraulic impact (described by the Hagen-Poiseuille law) a small-scaled analysis of the wettability of soils (or of related parameters, i.e., the PWI) is useful for characterizing hydraulic properties of pore walls. To the best of our knowledge, this is the first work that supplies results for PWI on two different scales (spatial resolution ranging from 0.018 to 0.79 mm^2).

2. Material and Methods

2.1 Soil material and sampling

In total 72 soil cores were excavated in September 2014 from a Haplic Luvisol (IUSS Working Group WRB, 2006) at the experimental area of Campus Klein-Altendorf (50°37'9'' N 6°59'29'' E, University of Bonn, Germany). The site is characterized by a maritime climate with temperate humid conditions (9.6°C mean annual temperature, 625 mm annual rainfall). Some main soil properties are listed in Table 1. The Bt horizon is characterized by accumulated clay, leached from the A-horizon (0-0.27 m) and the E horizon (0.27-0.41 m).

The soil samples were excavated from four pits (see Table 1) of a totally randomized trial (Kautz et al., 2014). Chicory (*Cichorium intybus* L. 'Puna', 5 kg ha^{-1} seeding rate) had been grown in these trials for the last three years. With its herringbone or monopodial branching root systems *Cichorium intybus* L. is known for its ability to penetrate deeply into the subsoil exploring for water and nutrient supply (Kautz et al., 2012). After the roots decay, large (diameter ≥ 5 mm), continuous biopores remain that can potentially be colonised by earthworms. Soil samples from two layers within the Bt-horizon (0.41-1.15 m) were investigated: Bt-1 from 0.45-0.55 m and Bt-2 from 0.55-0.65 m depth.

From both horizons soil cores of 3 cm in diameter, and 10 cm in height were excavated such that each core contained a macroscopic biopore (≥ 5 mm in diameter). The type of the biopore was classified endoscopically (Kautz et al. 2015) according to its "History" as either:

- Colonized and/or created by a plant root (*Cichorium intybus* L., (R))
- Colonized and/or created by an earthworm (*Lumbricus terrestris*, (EW))
- Colonized and/or created by a plant root followed by short-term colonisation of *L. terrestris*, (REW).

The latter one had been colonized by earthworms for a period of approximately six months. Earthworms were fed with ryegrass residues placed at the soil surface in this period. Before sampling, the epi-earthworms were removed with the octet method (Thielemann, 1986).

Since *L. terrestris* was the only deep-burrowing earthworm present at the studied site all earthworm burrows were formed by this species. The sample cores were first equilibrated to a defined matric potential of (Ψ_m = -30 kPa, equals field capacity), and

scanned with a micro X-ray computed tomograph (µCT Nanotom© 180; GE Sensing & Inspection Technologies GmbH, Wunstorf, Germany). *Afterwards, sub-samples were saturated again, and drained to defined matric potentials (i.e., Ψ_M = -1kPa; -3 kPa; -6 kPa - using sand beds - or -30 kPa – with the help of ceramic plates. See Haas et al 2016 for more information) for sorptivity measurements described later.*. Sub-samples were cut off vertically (Fig. 1) using a scalpel for all measurements. Sub-samples were stored at 4°C prior to the initial equilibration and before diffuse reflectance infrared Fourier transform spectroscopy.

2.2 Some soil properties

Disturbed, air-dried, and sieved soil (< 2 mm) was used for standard soil parameters. pH values were determined in 25 ml 0.01 M $CaCl_2$ (1:2.5 m/v, Blume et al., 2010). Inorganic carbon was determined by Scheibler analysis (Blume et al., 2010). Soil organic carbon (SOC) content was calculated by subtracting the inorganic carbon concentration from total carbon concentration determined via dry combustion at 1200 °C (Coulomat 702, Ströhlein instruments, Kaarst, Germany; Schlichting et al. 1995). Soil texture was determined according to Schlichting et al. (1995) by combined sieving and sedimentation processes (pipette method) after removal of cementing substances (HCl to remove $CaCO_3$; H_2O_2 for organic carbon oxidation; Na-pyrophosphate for dispersion).

*2.3 Diffuse reflectance infrared Fourier transform (*DRIFT*) spectroscopy*

The preparation of the equilibrated sub-samples for DRIFT spectroscopy required a thickness reduction of the sub-samples by scraping off material from the external side of the soil column such that the samples thickness was about 0.01 m. The obtained thin intact soil samples were wrapped in tin foil (Ellerbrock et al., 2009) and fixed on aluminium plates - with the external side located towards the aluminium plate. These thin intact soil samples were air-dried and stored in a desiccator over dried silica gel for 16 hours, before DRIFT spectroscopy was performed. Measurements were performed at two scales:

(i) The DRIFT mapping technique **(macro-DRIFT**) performed with a Bio-Rad FTS 135 (BioRad Corp, Hercules, CA, USA) combined with an XY-positioning table (Pike,

Madison, USA, adapted by Resultec, Illerkirchberg, Germany). The DRIFT mapping was carried out along transects across the biopores in 1 mm steps (Fig. 2; transect length is the whole sample width). Here, two transects of each of four samples, were investigated per history and depth. The IR beam was separately focused at each measurement point with respect to surface elevation (Leue et al., 2013) to avoid micro-topography effects on the spectra (Leue et al., 2011). Each macro-DRIFT spectrum was recorded by 16 co-added scans.

(ii) DRIFT microscopy **(micro-DRIFT)** used a Cary 660 combined with a Cary 610 microscope (both from Agilent Technologies, Santa Clara, CA, USA). Transects that cover the first 2.5mm next to the biopore wall were measured in 0.15 mm steps (see scheme in Fig. 2). Two transects of each of two samples, were investigated per history and depth. For the micro DRIFT measurements, no separate focussing of each measurement point was done to ensure that the IR beam meets its designated position. Each spectrum obtained by micro DRIFT was recorded by 32 co-added scans.

All DRIFT spectra, micro and macro, were recorded in a range of 400–4000 cm^{-1}, with a resolution of 1 cm^{-1} (FTIR) (Ellerbrock et al., 1999), and corrected against ambient air as background (Haberhauer and Gerzabek, 1999) by using a gold target (99% Infragold©, Labsphere, North Sutton, NH, USA) that was fixed onto the positioning table at the average sample surface elevation. Note, for macro DRIFT the diameter of the IR beam is about 1 mm (i.e, an area of 0.8 mm^2) while for micro DRIFT it is about 0.15 mm (i.e., an area of about 0.02 mm^2) (Table 2). Therefore, the area of a single measurement point investigated by macro DRIFT was about 40 times larger than that observed with micro DRIFT.

All spectra were transformed into Kubelka-Munk (KM, Kubelka 1948, Kubelka and Munk 1931) units using the software WIN-IR Pro 3.4 (Digilab, MA, USA), baseline corrected, smoothed (boxcar, factor 15), and zapped for absorptions bands associated with carbon dioxide (WN regions 2386-2297 cm^{-1}). Spectra from equidistant measurement-points along transects were pooled, resulting in a much higher number of replicates for the surface of the biopore samples. The C-H band intensities of the DRIFT spectra – characteristic for hydrophobic alkyl groups in OM - were measured as a vertical distance (i.e., as height) from a local baseline plotted between tangential points in the spectral regions between WN 2948 - 2920 cm^{-1} and

2864 - 2849 cm^{-1} (Table 2). The C=O band intensities (i.e., characteristic for hydrophilic alkyl groups in OM) were measured as height from the total baseline of the spectra in the regions of WN 1720 - 1700 cm^{-1} and 1625 - 1600 cm^{-1}). The potential wettability index (PWI; Leue et al., 2013) used to characterize the organic matter was calculated as the ratio between the summed C-H signal intensities and the summed C=O signal intensities (C-H/C=O ratio; Ellerbrock et al., 2005). Larger PWI values indicate a smaller potential wettability of the OM.

2.4 Soil water repellency

Soil wettability was measured using a range of approaches (summarized in Table 3). (I.) An optical method provided the direct contact angle of intact soil samples by measuring the angle of a water droplet deposited on the soil surface by a syringe positioned above the sample. A high-speed camera (OCA20, DataPhysics, Filderstadt, Germany) with a frame rate of 250 s^{-1} was used to record droplet dynamics. SCA20 software (DataPhysics, Filderstadt, Germany) was used for analysing and calculating contact angles. The soil samples' surface is not flat, which is especially true for the surface of biopores. To determine the contact angle correctly we cut the samples into much smaller sub-samples (≤ 5 mm thick x 10 mm x 10 mm), aiming to achieve plain sections. Air-dried sub-samples were fixed to an aluminium plate. The left- and right-handed side contact angles of each droplet were averaged. Measurements were replicated 3 times for each sample and each zone (bulk or biopore). Each droplet had a volume of around 8 µl. Under the assumption of a ball-shaped droplet its extension in area is ≥4 mm^2. Thus, this method showed the lowest spatial resolution applied on structured soils in this study. The used water was stored in vacuum to reduce the amount of dissolved gases in the liquid.

(II.) Wettability was also quantified from sorptivity tests at a hydraulic gradient of +0.02 m, as described in Hallett et al. (2003). Instead of a sponge filled tube, we used a smaller capillary (Minicaps, 5 µL, Hirschmann Laborgeraete, Germany, ISO 7550) to gather infiltration rates of both, water and ethanol successively with a spatial resolution of around 0.1 mm^2. Liquid uptake by the soil from a reservoir was recorded for 90 seconds every 1 second from a 0.1 mg balance. Sorptivity S (m s$^{-0.5}$) was calculated according to Eq. 1 (Hallett et al. 2003):

$$S = (Q \cdot f \cdot (4 \cdot b \cdot r)^{-1})^{0.5} \qquad\qquad \text{(Eq. 1)}$$

where Q is the liquid flow rate ($m^3 s^{-1}$), f is the fillable air-porosity (-) f (Leeds-Harrison et al., 1994), b accounts for the wetting front and was assumed to be 0.55, and r is the diameter of the used capillary (m). The contact angle, CA from sorptivity tests was calculated by:

$$CA = \arccos \left(1.95 \cdot S_{ethanol} \cdot S_{water}^{-1} \right)^{-1}$$ (Eq. 2)

(III.) Measurements with the Wilhelmy plate method were performed on homogenized soils that were passed through either a 2 mm (Fig. 6a) or 0.63µm (Fig. 6b) sieve. The measurements were conducted as described in Goebel et al. (2008) and transformed to CA using calculations from Bachmann et al. (2003). We used a microtensiometer (Kruess, Hamburg, Germany) fitted with a Peltier element to maintain the temperature of the deionised water as wetting fluid at 20°C. The Wilhelmy plate method provides both advancing and receding CAs, whereas most other methods only provide the advancing CA. Three replicates were measured for the bulk soil. As the method needs relatively large amounts of soil for a single measurement, we were not able to investigate biopore wall-borne soil. The CA (θ) was calculated according to Bachmann et al. (2003) from the force F (N) acting on the plate using Eq. (3):

$$\cos \theta = F \cdot (\rho \cdot \sigma_{LV})^{-1}$$ (Eq. 3)

with density ρ ($Mg\ m^{-3}$) and surface tension of the wetting liquid σ_{LV} ($N\ m^{-1}$). The latter was determined using a microtensiometer and a platinum plate. The calculation according to Eq. 3 is based on an assumed complete wettability of the platinum plate ($\cos \theta = 1$). For more details see Holthusen et al. (2012).

2.5 Statistical analyses

The statistical software R (R Development Core Team, 2017) was used for plotting and evaluating the results. Contact angles as derived from sessile drop method, from the Wilhelmy plate method, or from sorptivity tests, as well as, water and ethanol sorptivity data, and the log-transformed PWI values were analysed with R software analogously.

The data evaluation started with the definition of an appropriate statistical mixed model (Laird and Ware, 1982; Verbeke and Molenberghs, 2000). Data were tested for normality and for homoscedasticity. These assumptions are based on a

graphical residual analysis. The statistical model included (i) the history of the biopore (as shown in section 2), (ii) the sampling depths (0.45-0.55 m and 0.55-0.65 m), (iii) the distance from the biopore surface and the (iv) pit (1-4), as fixed factors. The considered covariates (shown in Table 1 and their potential interaction effects) are based on a model selection, resulting in equations as follows:

$$PWI_{ij} = e^{a_{ij}* pH_{ij}} * e^{b_{ij}* dist} * e^{c_{ij}} \qquad \text{(Eq. 4)}$$

with *a,b*, and *c* as fitting parameter, *i* and *j* define the histories of the biopores and the depths, and *dist* the distance from the biopore surface (10^{-3} m). e is Euler's number.

The random effects were defined by the plots and suitable interaction effects with history, depth and cylinder, assuming a split-plot design (pit + pit:history + pit:history:depth + pit:history:depth:cylinder + residual error). Based on this model, a Pseudo R^2 was calculated (Nakagawa and Schielzeth, 2013) and an analysis of covariance (ANCOVA) was conducted (Cochran, 1957).

3. Results

For texture and soil organic carbon-content, no depth-dependent trends were found (Table 1), while pH increased slightly with depth.

3.1. Organic matter composition and water repellency

Absorption bands of hydrophobic C-H groups (wavenumber (WN) 2948–2920 cm^{-1} and WN 2864–2849 cm^{-1}) were easily detectable in the spectrum of the biopores' surface and, especially, in the spectrum of POM (Fig. 2: blue line), but almost undetectable in the spectrum of the soil matrix (Fig. 2: grey line). Furthermore, the DRIFT spectra of POM were mostly not affected by so called "bulk mode bands" (2000 – 1700 cm^{-1}, Ellerbrock et al. 2016), caused by lattice vibrations in soil minerals (i.e., quartz) if those particles have diameters above 70 µm (Leue et al., 2010a).

Since equidistant measurement-points (i.e., with same distance from the surface of the biopore wall) were pooled at the macro scale (Fig. 3a) a much larger number of measurement points were considered for characterizing the biopore surface. The PWI values obtained from macro DRIFT analysis showed highest

means for the biopore surfaces (distance = 0 mm) and decreased with increasing distance from the biopore wall. The relatively high standard deviations for PWI (macro DRIFT) indicate a large heterogeneity in quality and quantity of SOM distributed at the biopore surfaces. The PWI was found to scatter within 5 and 8 mm distance for the R-samples from Bt2, within 1-3 mm distance for the EW-samples from Bt-1 or within the 0-9 mm distance for the R-samples from Bt-1 and for both depths for the REW samples.

On the micro scale (Fig. 3b) the largest means of PWI were documented within some distance from the biopores surface: for the R-samples from Bt-1 two peaks in PWI were exhibited in 0.5 and 1.5 mm distance from the surface and smaller means for PWI from Bt-2. Pores colonized by earthworm showed larger values within 0 to 1.5 mm (Bt-1) or 0 to 0.6 mm (Bt-2) in distance from the biopores' surface. Values for REW from Bt-1 showed the most pronounced scattering with its maximum in 0.15 mm distance from the biopores' surface or an almost absence of larger PWI values within 1.5 mm in distance from the biopores surface and a peak in 1.75 mm (Bt-2). On the micro scale, REW showed the smallest depth-dependent means for the PWI of all biopore histories.

The statistical analysis of covariance (see section 2.5) showed significant interactions for the logarithmic PWI between the history, the distance and the depth on the micro scale. At the macro scale, the influence of the pH value improved the statistical model, additionally. Table 4 shows the regression coefficients for macro scale which can be used with Eq. 4. . Since the statistical analysis for results of the sessile drop method showed that the sampling zone (matrix or biopore) was the only significant influence on contact angles, we pooled the biopores' histories (Fig. 4). This resulted in 8 points for each zone (biopore and bulk), each representing a single depth of each pit. In Figure 4 the PWI is plotted against the contact angle as derived from the sessile drop method (Fig. 4a) or sorptivity tests (Fig. 4b). The sessile drop method delivered promising results with highly significant differences between biopores and bulk soil. Here, the means of the bulk soil contact angles are close to 30° and could be determined with good repeatability as indicated by the small standard deviations. The biopores' heterogeneity is reflected by means of contact angles between 55° and 85°.

CA derived from sorptivity tests (Fig. 4b) differed from those of the sessile drop and no clear statistical influence of the type of surface (matrix or biopore) was found. There were only weak ($0.05 \leq p \leq 0.1$) significant interactions between the CA and matric potential, the measurement zone and the pit the soil cores were from. The CA values derived from sorptivity tests ranging from $46.9° \pm 29.1°$ to $70.3° \pm 6.4°$ (Table 5) of matrix surfaces are not significantly different from those of biopore surfaces (ranging from $48.8° \pm 17.1°$ to $75.2° \pm 4.6°$). The same is found for the water sorptivity (Fig. 5), which ranged from 0.002 to 0.07 mm $\cdot$ s$^{-0.5}$. However, general trends could be observed: With decreasing water content (decreasing matric potential) scattering and water sorptivity increases while differences in median between matrix and biopore surfaces disappear. Note, pores colonized by earthworms (i.e., EW; Ψ_m = -1 kPa, and REW; Ψ_m = -3 kPa), show a good repeatability for sorptivity data.

The CA values as derived from the Wilhelmy plate method ranged from $38.4°$ to $66.6°$, if the soil is sieved to ≤ 2 mm (Fig. 6a) or from $30.4°$ to $52.9°$ if the soil is sieved to ≤ 0.63 mm (Fig. 6b). Although the latter one showed a good repeatability indicated by lower standard deviations the values were not different for biopore as compared to matrix surface samples.

4. Discussion

The presented water sorptivity rates are more than ten times lower than those shown by Hallett et al. (2003) who investigated soil from both, the rhizosphere and bulk soil at different water contents. However, in contrast to Hallett et al. 2003, who used an infiltrometer device with 0.4 mm in diameter, the infiltrometer tip used here show a diameter of about 0.22 mm. Note, as stated by Hallett et al. 2003, the sorptivity rates should decrease with decreasing diameter of the infiltrometer tip which is in accordance to the ten times lower sorptivity rates found here. The larger repeatability of the water sorptivity rates (Fig. 5) for the surface samples from EW and REW could be explained by homogenization caused by the earthworms' activity. However, differences in water transport were not statistically significant. These differences could be caused by two processes: (i) the colonizers' influence on aggregation and (ii) exudates and secondary metabolites (Hallett et al., 2003) because they may coat soil particles and induce slightly higher water repellency in the outermost layer of

biopore samples (Czarnes et al., 2000). The influence of such outermost layers could be shown by comparing samples ≤ 2 mm (Fig. 6a) with those ≤ 0.63 mm (Fig. 6b). By sieving the soil to 0.63 mm aggregates > 0.63 mm were destroyed and therewith their organic coatings, leading to a more homogenous soil. This homogenization resulted in lower means and standard deviations (effect of dilution of hydrophobic substances). It could be assumed that the hydrophobicity of the aggregate coatings is mostly caused by two processes: (i) the accumulation of amphiphilic organic substances which are not able to diffuse into the aggregates' interior due to their size and (ii) due to differences in the spatial orientation of SOM functional groups caused by the dual porosities of soils (aggregates' in- and exterior pore space): If a water saturated soil dries its drainage starts with its largest pores. In this case the hydrophobic functional groups of SOM are orientated towards air-filled pores, while the hydrophilic functional groups are orientated towards the soil water (Bachmann et al., 2003). The largest pores are mostly biopores, while coarse pores are found at the interaggregates' pore space, which is located next to the aggregates' exterior. The smallest pores were found at the aggregates' interior. Since some of these pores never dried, this change in the spatial orientation of the hydrophilic groups in SOM towards the mineral particles is not forced as it is for the larger pores, resulting in lower CA. However, the results for the homogenous soil fit well to those gathered from the sessile drop method.

As in Leue et al. (2010b; 2013) and Fér et al. (2016), we found larger PWI values for the surfaces of root channels and earthworm burrows, as compared to the matrix (i.e., surrounding soil). Such higher PWI values are also related to a lowered wettability of these regions, described by increased contact angles (Leue et al., 2015) resulting in decreased infiltration rates (Hallett et al., 2003). The lower wettability of the biopore surfaces may be caused by the accumulation of organic components (like plant waxes or terpenes) which originate from earthworms or roots by release and / or illuvial processes and perfectly follows the enlarged transportability of these organic compounds, caused by increased diffusion coefficients in biopore walls compared to soil matrices as found by Koebernick et al. (2017) and Haas et al. (unpublished).

The PWI values determined from macro DRIFT spectra of earthworm (EW) burrow walls are similar to those of the root channels (R) (Fig. 3a) but larger than those of root channel surfaces recolonized by *L. terrestris* (REW), while PWI values

determined from micro DRIFT spectra indicate a strong decrease in PWI for the REW from Bt-2 as compared to R and EW samples (Fig 3b). Two processes may be responsible: an enhanced mechanical redistribution of organic particles caused by a total loss of soil aggregation, which may be the result from shearing forces exerted by earthworm movements through thickening and following sliding through the cracking soil volume at high water contents. Because of homogenisation caused by the earthworm´s activity, regions with higher means in PWI (surface of biopores and/or exterior of aggregates) are mixed with regions of low PWI (soil matrix and/or interior of aggregates) resulting for REW samples in PWI values lower than for EW and R samples. We expect the homogenization potential of a moving earthworm to be larger at biopores that had been colonized by plant roots prior to earthworm colonization, because plant roots alter the soil surface chemically and physically (Ruiz et al., 2015). Exudates increase the water content at given matric potential, nutrient uptake affects the surface charge and pH apart from a physical pore-size shift, and altered pore geometry (Whalley et al., 2005). Consequently, the decay of organic particles should be enhanced in biopores colonized by both, EW and R, since such biopores show pH values more favourable for microorganisms than biopores colonized by R or EW alone (Whalley et al. 2005). Biopores colonized only by roots will be more acidic due to CO_2 and H^+ release while those colonized solely by EW will result in a more alkaline soil due to calcite release from specialized oesophageal glands (Lankester, 1865).According to DRIFT data the zone of the biopore walls influenced either by EW, R or REW is limited to a thickness of about 0-2 mm which is in accordance with Koebernick et al. (2017), Uteau et al. (2015) and Leue et al. (2010). For biopores created by EW and REW the PWI values became relatively constant (i.e., small standard variations) for zones that are in distances above 2 mm from the biopore wall (Fig. 3), whereas the PWI for <2 mm in distance from the pore wall surface indicated the formation of a kind of lining. Such trend was especially detectable with micro-DRIFT technique (micro scale, Fig. 3b) for EW biopores. However, for the R-biopores at distances above 2 mm strong variations in PWI values were found at both, macro and micro, scale. Such stronger variation in PWI for the R-biopores may be explained by effects of lateral roots growing into the soil matrix surrounding the root channel. Differences in the width of the earthworm linings (0 to 1.5 mm for Bt-1 and 0 to 0.6 mm for Bt-2), can be explained by a higher

energy needed for the mechanical work to extent the cavity with increasing soil depths (as described by Mohr-Coulomb theory, Horn et al., 1994; Ruiz et al., 2015).

The results of sorptivity test and sessile drop procedure (Fig. 4) confirmed the PWI determined from DRIFT spectra, indicating a reduced wettability for biopore walls. This is in accordance with findings of Hallett et al. (2003) using sorptivity tests, and with those of Leue et al. (2015) using sorptivity tests and sessile drop method.

Differences between the results of the three different CA measurement methods and the PWI are caused by (i) the different spatial resolutions and (ii) methodological limitations of the used techniques, as well as by (iii) differences in sample preparation (intact, and sieved samples). Using the identical technique, the obtained results are albeit different because of the spatial distribution of organic components such as SOM at surfaces of intact soil samples. It is distributed mostly heterogeneous (i.e., patchy layers Kaiser and Guggenberger, 2000) and has especially with a highly sensitive method a large impact on the measured parameters (e.g., PWI values of micro vs macro DRIFT) .If different methods are used and the results compared (ii), also different results will be obtained for sorptivity tests since these procedures are mostly limited to samples that show CA smaller than 90° because the samples need to be wettable to a certain extent (Bachmann et al., 2003). In contrast the sessile drop and the Wilhelmy plate method both allow to analyse samples with CA from 0 to 180°. Cosentino et al. (2010) compared different methods for assessing the wettability of soils (namely sorptivity tests, capillary rise method and water droplet penetration time test), and stated that these methods measure different related soil properties. In soils with small levels of water repellency, water droplet penetration time test (WDPT) determines the rate of wetting by water, whereas the R index (calculated from sorptivity tests) and CRM measure hydrophobicity. Furthermore, the sorptivity test uses two wetting liquids, with ethanol potentially mobilising organic compounds, changing pore surface roughness and causing differences in swelling at the wetting front compared to water. Furthermore (iv), as Leue et al., 2010b stated, the CA is characterized by the first contact of a droplet at a sample surface, thus, the OM properties of the outermost surface molecules are of essential importance (Bachmann et al., 2003). Fungal hyphae are e.g. known for their hydrophobicity. In this study the maximum CA of about 132° was measured (sessile drop method) directly at a fungal mycelium. Such data shows extreme hydrophobic behaviour while fungal hyphae can be also partly hydrophilic as well which was observed by

goniometer measurements in this study. Such hyphae were roped into a water droplet, followed by a release of spores. The processes result in smaller CA values. Additionally inconsistences between CA and PWI data are probably caused by the penetration depth of the IR radiation of about 6 to 8 μm that strongly exceeds the thickness of the outermost molecular OM layer (Diehl, 2013). The results show, that the extent of water repellency of a biopore wall finally depends on their colonization history (root and/or earthworm) and on the soil depths and is much more pronounced in biopore walls than it is in the soil matrix. Therewith, the capillary rise or the water-content at a given matric potential is lowered (described by Jurin's law) and so is the flow of water through the biopore wall at a given matric potential. However, small-scaled (micro) DRIFT measurements showed, that even if macro DRIFT measurements indicate pronounced water repellency, biopore walls can have a certain surface percentage with less pronounced water repellency. These regions act as preferential flow paths from the biopore wall into the soil matrix. Finally, we also need to consider the time-dependency or reversibility of the water repellency which affects the water flow during an event of precipitation. However, until now, these dynamic processes are neither completely understood nor have interactions between the composition of mineral surface layers and time dependent alterations of water repellence been quantified. Further research should therefore focus on the dynamics of OM quality and water repellency in biopore walls and their surrounding soil matrixes. The repeated analyzation of defined loci of artificial pores which could be colonized by an earthworm and/or root at defined time points during the recolonization would eliminate the influence of soil heterogeneity.

5. Conclusion

1) The contact angle, the PWI, and with that the chemical composition of biopore walls differed from the soil matrix. Furthermore, the spatial extent of the alteration of the soil depends on the biopores' colonizer (root, earthworm or both) and on further soil factors like soil depth.

2) Results showed that SWR is heterogeneous distributed at transects across biopores. Thus, water flow is expected to occur preferentially through regions with a less pronounced SWR.

3) The linkage of PWI values to contact angles gathered from other methods (especially from the sessile drop method / optical measurements) delivered promising results despite of methodologically given differences in spatial resolution.

4) The DRIFT spectroscopy is an easy, fast, and reliable method that allows feedbacks on the chemical composition of the organic coatings of surfaces. Its potentially high spatial resolution and its broad field of application make the DRIFT spectroscopy a highly appropriate approach in small-scaled soil analysis. However, the PWI a dimensionless parameter indicates only a potential for water driven transport but did not reflect real transport functions.

5) Further research is needed to derive transfer functions that link PWI values with wettability properties like CA.

6) Earthworm activity was found to reverse the reduced wettability (in terms of high means in PWI) of biopore walls, resulting in lower CA and therewith higher infiltration rates into the surrounding soil which in turn leads to a larger amount of water available for plant production. Consequently, we suggest an increase of both, the number of deep rooting plants in crop rotation, and the number of individuals of earthworms to optimize water transport or even capillary rise through agricultural soils with respect to sustainable agricultural productivity. This can be justified using Good Agricultural Practices (GAP).

Acknowledgments

Literature

Bachmann, J., Woche, S. K. & Goebel, M.-O. (2003). Extended methodology for determining wetting properties of porous media. Water Resour. Res. 39, DOI: 10.1029/2003WR002143.

Blume, H.-P., Stahr, K. & Leinweber, P. (2010). Bodenkundliches Praktikum. Spektrum, Heidelberg.

Bossuyt, H., Six, J. & Hendrix, P. F. (2005). Protection of soil carbon by microaggregates within earthworm casts. Soil Biol. Biochem. 37:251–258.

Carvalhais, L. C., Dennis, P. G., Fedoseyenko, D., Hajirezaei, M.-R., Borriss, R., von Wiren, N. (2011). Root exudation of sugars, amino acids, and organic acids by maize as affected by nitrogen, phosphorus, potassium, and iron deficiency. J. Plant Nutr. Soil Sci. 174:1‑9.

Christiansen-Weniger, C., Groneman, A. F. & van Veen, J. A. (1992). Associative N_2 fixation and root exudation of organic acids from wheat cultivars of different aluminium tolerance. Plant Soil, 139:167–174.

Cosentino, D., Hallett, P. D., Michel, J. C. & Chenu, C. (2010). Do different methods for measuring the hydrophobicity of soil aggregates give the same trends in soil amended with residue? Geoderma 159(1-2): 221-227.

Czarnes S., Hallett P.D., Bengough A.G. & Young, I.M. (2000). Root- and microbial-derived mucilages affect soil structure and water transport. Eur. J. Soil Sci. 51: 435–443.

Diehl, D. (2013). Soil water repellency: Dynamics of heterogeneous surfaces. Colloids Surf., A 432, 8–18.

Doerr, S. H., Shakesby, R. A. & Walsh, R. P. D. (2000). Soil water repellency: its causes, characteristics and hydro-geomorphological significance. Earth-Sci. Rev.51:33–65.

Ellerbrock, R. H. & Gerke, H. H. (2004). Characterizing organic matter of soil aggregate coatings and biopores by Fourier transform infrared spectroscopy. Eur. J. Soil Sci. 55:219–228.

Ellerbrock, R. H., Gerke, H. H., Bachmann, J. & Goebel, M.-O. (2005). Composition of organic matter fractions for explaining wettability of three forest soils. Soil Sci. Soc. Am. J. 69:57–66.

Ellerbrock, R. H., Gerke, H. H. & Böhm, C. (2009). In situ DRIFT characterization of organic matter compositions on soil structural surfaces. Soil Sci.

Soc. Am. J. 73:531–540.

Ellerbrock, R. H., Leue, M. & Gerke, H. H. (2016). Interpretation of infrared spectra for OM characterization of soil structural surfaces of Bt-horizons. J. Plant Nutr. Soil Sci., 179:29–38.

Fér, M., Leue, M. , Kodešová, R., Gerke, H.H. , R. H. Ellerbrock. (2016). Droplet infiltration dynamics and soil wettability related to soil organic matter of soil aggregate coatings and interiors. J. Hydrol. Hydromech., 64, 2016, 2, 111–120.

Haas, C., D. Holthusen, A. Mordhorst, J. Lipiec, R. Horn. 2016. Elastic and plastic soil deformation and its influence on emission of greenhouse gases. Int. Agrophys., 30, 173-184.

Hallett, P. D., Gordon, D. C. & Bengough, A. G. (2003). Plant influence on rhizosphere hydraulic properties: direct measurements using a miniaturized infiltrometer. New Pythol. 157:597-603.

Hoang, D. T. T., Pausch, J., Razavi, B. S., Kuzyakova, I., Banfield, C. C. & Kuzyakov, Y. (2016). Hotspots of microbial activity induced by earthworm burrows, old root channels, and their combination in subsoil. Biol Fertil Soils (2016) 52:1105–1119.

Holthusen, D., Haas, C., Peth, S. & Horn, R. (2012). Are standard values the best choice? A critical statement on rheological soil fluid properties viscosity and surface tension. Soil Till. Res. 125: 61-71.

Horn, R., Taubner, H., Wuttke, M. & Baumgartl, T. (1994). Soil physical properties related to soil structure. Soil Till. Res. 30 (1994) 187-216.

Jarvis, N. J. (2007). A review of non-equilibrium water flow and solute transport in soil macropores: Principles, controlling factors and consequences for water quality. Eur. J. Soil Sci. 58:523–546.

Jones, D. L., Nguyen, C., Finlay, R. D. (2009). Carbon flow in the rhizosphere: carbon trading at the soil-root interface. Plant Soil 321:5‑33.

Kaiser, M., Ellerbrock, R. H. & Gerke, H. H. (2008). Cation exchange capacity and composition of soluble soil organic matter fractions. Soil Sci. Soc. Am. J. 72:1278–1285.

Kaiser, M. & Guggenberger, G. (2000). The role of DOM sorption to mineral surfaces in the preservation of organic matter in soils. Org. Geochem. 31:711-725.

Kautz, T., Amelung, W., Ewert, F., Gaiser, T., Horn, R., Jahn, R., & Köpke, U. (2012). Nutrient acquisition from arable subsoils in temperate climates: A review. Soil Biol. Biochem., 57:1003-1022.

Kautz, T., Lüsebrink, M., Pätzold, S., Vetterlein, D., Pude, R., Athmann, M., Küpper, P. M., Perkons, U. & Köpke, U. (2014). Contribution of anecic earthworms to biopore formation during cultivation of perennial ley crops. Pedobiologia 57:47–52

Koebernick, N., Daly, K. R., Keyes, S. D., George, T. S., Brown, L. K., Raffan, A., Cooper, L. J., Naveed, M., Bengough, A. G., Sinclair, I., Hallett, P. D. & Roose, T. (2017). High-resolution synchrotron imaging shows that root hairs influence rhizosphere soil structure formation. New Pythol. 216:124-135.

Kubelka, P. (1948). New contributions to the optics of intensely light-scattering materials. Part I. J. Opt. Soc. Am. 38:448–457.

Kubelka, P. & Munk, F. (1931). Ein Beitrag zur Optik der Farbanstriche. (In German.) Z. Tech. Phys. 11:593–601.

Kuzyakov, Y. & Blagodatskaya, E. (2015). Microbial hotspots and hot moments in soil: concept and review. Soil Biol Biochem 83:184–199.

Lankester, E.R. (1865). The anatomy of the Earthworm. J. Cell Sci. 1865 s2-5: 99-116.

Leue, M., Eckhardt, K.-U., Ellerbrock, R. H., Gerke, H. H. & Leinweber, P. (2016). Analyzing organic matter composition at intact biopore and crack surfaces by combining DRIFT spectroscopy and Pyrolysis-Field Ionization Mass Spectrometry. J. Plant Nutr. Soil Sci., 179:5–17.

Leue, M., Ellerbrock, R. H., Bänninger, D. & Gerke, H. H. (2010a). Impact of soil microstructure geometry on DRIFT spectra: comparisons with beam trace modelling. Soil Sci. Soc. Am. J. 74, 1976–1986.

Leue, M., Ellerbrock, R. H. & Gerke, H. H. (2010b). DRIFT mapping of organic matter composition at intact soil aggregate surfaces. Vadose Zone J. 9, 317–324.

Leue, M., Gerke, H. H. & Ellerbrock, R. H. (2013). Millimetre-scale distribution of organic matter composition at intact biopore and crack surfaces. Eur. J. Soil Sci. 64, 757–769.

Leue, M., Gerke, H. H. & Godow, S. (2015). Droplet infiltration and OM composition of intact crack and biopore surfaces from clay-illuvial horizons. J. Plant Nutr. Soil Sci. 178, 250–260.

Moody, D. R., & Schlossberg, M. J. (2010). Soil Water Repellency Index Prediction Using the Molarity of Ethanol Droplet Test. Vadose Zone J. 9, 1046–1051

Nunan, N., Wu, K., Young, I. M., Crawford, J. W. & Ritz, K. (2003). Spatial distribution of bacterial communities and their relationships with the micro-architecture of soil. FEMS Microbiol. Ecol. 44, 203– 215.

Peng, X. & Horn, R. (2005) Modelling Soil Shrinkage Curve across a wide range of Soil Types. SSSAJ. 69:584-592.

R Development Core Team. (2017) R: A language and environment for statistical computing. R Foundation for Statistical Computing, Vienna, Austria. ISBN 3-900051-07-0, URL http://www.R-project.org/

Ruiz, S., Or, D. & Schymanski, S. J. (2015). Soil Penetration by Earthworms and Plant Roots—Mechanical Energetics of Bioturbation of Compacted Soils. PLoS ONE 10(6): e0128914.

Scheu, S. (1991) Mucus excretion and carbon turnover of endogeic earthworms. Biol. Fertil. Soils. 12:217-220.

Schlichting, E., Blume, H.-P. & Stahr, K. (1995). Bodenkundliches Praktikum. Blackwell Wissenschafts-Verlag, Berlin, Wien.

Six, J., Frey, S.D., Thiet, R.K., & Batten, K.M. (2006). Bacterial and fungal contributions to C-sequestration in agroecosystems. Soil Sci. Soc. Am. J., 70:555-569.

Six, J., Bossuyt, H., Degryze, S. & Denef, K. (2004). A history of research on the link between (micro)aggregates, soil biota, and soil organic matter dynamics. Soil Till. Res. 79:7–31.

Sizmur, T., Watts, M. J., Brown, G. D., Palumbo-Roe, B. & Hodson, M. E. (2001). Impact of gut passage and mucus secretion by the earthworm Lumbricus terrestris on mobility and speciation of arsenic in contaminated soil. J Hazard Mater. 197:169-175.

Thielemann, U. (1986). Elektrischer Regenwurmfang mit der Oktett-Methode. Pedobiologia 23:175-188.

Urbanek, E., Walsh, R. P. D. & Shakesby, R. A. (2014). Patterns of soil water repellency change with wetting and drying: the influence of cracks, roots and drainage conditions. Hydrol. Process. Vol. 29, 12:2799-2813.

Uteau, D., Hafner, S., Pagenkemper, S. K., Peth, S., Wiesenberg, G. L. B., Kuzyakov, Y. & Horn, R. (2015). Oxygen and redox potential gradients in the rhizosphere of alfalfa grown on a loamy soil. J. Plant Nutr. Soil Sci., 178: 278–287.

Vetterlein, D. & Marschner, H. (1993). Use of a microtensiometer technique to study hydraulic lift in a sandy soil planted with pearl millet (Pennisetum americanum [L.] Leeke). Plant Soil 149:275-282, 1993.

Whalley, W. R., Riseley, B., Leeds-Harrison, P.B., Bird N.R.A., Leech, P.K. & Adderley, W.P. (2005). Structural differences between bulk and rhizosphere soil. Eur. J. Soil Sci. 56:353-360.

WRB, 2006. World reference base for soil resources, FAO. ed, World Soil Resources Reports No 103. Rome.

Zheng, W., Morris, E. K., Lehmann, A., & Rillig, M. C. (2016). Interplay of soil water repellency, soil aggregation and organic carbon. A meta-analysis. Geoderma 283:39-47.

Fig. 1: Sample preparation and exemplary transect (yellow, dotted line). Samples were cut off vertically, air-dried and stored in a desiccator overnight, before Diffuse Reflectance Infrared Fourier Transform Spectroscopy (DRIFTS) was performed along the transects. Results of measurements at the biopores' surface were pooled (=0 mm distance to biopore surface, **Fig. 3** and **Fig. 4**). The same was done for equidistant measurement points.

Fig. 2: Exemplary spectra as derived from macro diffuse reflectance infrared Fourier transform (macro DRIFT) spectroscopy for particulate organic matter (POM (i.e., straw residues; blue line), for soil matrix close to biopore surface (yellow line) as well as for the soil matrix more distant (grey line) to biopore surface. The right-hand side shows transects at biopore samples studied by macro- and micro-DRIFT spectroscopy.

Fig. 3: Means and standard deviation for potential wettability index (PWI), derived from a) macro and b) micro diffuse reflectance infrared Fourier transform (DRIFT) spectra of biopores colonized and/or created by *Lumbricus terrestris* (EW), colonized and/or created by chicory (*Cichorium intybus L.*) roots (R), and biopores colonized and/or created by a plant root followed by colonisation of *L. terrestris* (REW). The upper row shows data for Bt-1 (0.45-0.55 m) while the lower row those for Bt-2 (0.55-0.65 m). PWI is defined as the ratio of the intensities of summed C-H signals to summed C=O signals. Results of measurements at the biopores' surface were pooled (=0 mm distance from biopore surface). The same was done for equidistant measurement points. For a) $n_{R,Bt-1}$ = 29,8,8,8,8,8,7,7,5,3; $n_{EW,Bt-1}$ = 37,8,8,8,8,8,8,8,6,4; $n_{REW,Bt-1}$ = 34,8,8,8,8,8,8,8,5,3; $n_{R,Bt-2}$ = 28,8,8,8,8,8,7,7,4,3; $n_{EW,Bt-2}$ = 33,8,8,8,8,8,8,8,5,6; $n_{REW,Bt-2}$ = 35,8,8,8,8,8,8,8,4,8. For b) n=4.

Fig. 4: Relation between potential wettability index (PWI) derived from macro diffuse reflectance infrared Fourier transform spectroscopy (Y-axis) and contact angles derived from a) optical measurements (sessile drop) on bulk soil (distance from biopore surface ≥ 5 mm, filled symbols) and biopore surface (blank symbols) or b) sorptivity tests. The biopores' histories were presented by differing symbols (R = triangle, EW = dots, REW = squares). Shown are arithmetic means with one standard deviation (solid line for Bt-1, dashed line for Bt-2). Results of measurements at the biopores' surface were pooled (=0 mm distance from biopore surface). Shown sorptivity data are for Ψ_m = -30 kPa, determined at a hydraulic gradient of +2 cm with an infiltrometer device, 0.22 mm in diameter. $n_{sorptivity}$ = 3.

Fig. 5: Influence of matric potential and zone (bulk soil or biopore with defined history (colonized and/or created by Lumbricus terrestris (EW), colonized and/or created by chicory (Cichorium intybus L.) root (R), as well as for biopores colonized and/or created by a plant root followed by colonisation of L. terrestris (REW)) on water sorptivity, determined at a hydraulic gradient of +2 cm with an infiltrometer device, 0.22 mm in diameter. $n_{sorptivity}$ = 3.

Fig. 6: Relation between potential wettability indexes (PWI) as derived from macro DRIFT spectroscopy and contact angles derived from Wilhelmy plate method for soil sieved to ≤ 2 mm (a) or ≤ 0.63 mm (b). Means with standard deviation for each depth and plot of the bulk soil (distance to biopore surface ≥ 5 mm). n_{WPM} = 3.

Table 1. Sand, silt, clay, as well as, soil organic carbon (SOC) contents in g kg^{-1} soil, as well as, pH, and electrical conductivity (eC) in µS cm^{-1} of the four pits where soil cores were excavated from a loess-derived Luvisol, Klein-Altendorf near Bonn, Germany.

Pit	Depth	Sand	Silt	Clay	SOC	pH	eC
	m		g kg^{-1}			-	µS cm^{-1}
24	0.45-0.55	71.4	780	149	4.0	7.0	83
24	0.55-0.65	66.1	730	204	5.8	7.03	74
40	0.45-0.55	54.7	650	295	4.5	6.99	100
40	0.55-0.65	44.8	710	245	3.4	7.11	83
57	0.45-0.55	59.8	770	170	3.9	7.02	81
57	0.55-0.65	44.6	740	215	4.1	7.0	71
74	0.45-0.55	58.9	660	281	4.0	6.98	104
74	0.55-0.65	40.0	700	260	3.8	7.02	77

Table 2. Details about diffusive reflectance Fourier transform infrared spectroscopy (DRIFTS) for measurements at microscale and macroscale. Macro-DRIFTS was performed with Bio-Rad FTS 135 (Bio-Rad, Munich, Germany), micro-DRIFTS with Cary 660 FTIR, connected to microscope model Cary 610 (microscope, Agilent Technologies, Santa Clara, CA, USA).

Parameter / Method	Macro-DRIFTS	Micro-DRIFTS
Investigated area (mm^2)	0.79	0.018
radii of IR beam (mm)	1	0.15
Max. distance to biopore (mm^{-1})	15	2.25
Smoothing factor (-)	15	
Wave number of functional groups (cm^{-1})		
C-H (asymmetric) "A"-band	2948–2920	
C-H (symmetric) "A"-band	2864–2849	
C=O "B"-band	1720–1700	
C=O "B"-band	1625–1600	

Table 3. Overview of the used methods and their spatial resolution.

	Sessile drop method (Goniometer)	Infiltration tests	Wilhelmy plate method	diffuse reflectance infrared fourier transform spectroscopy (DRIFTS)
Principle	Deposition of a water droplet, filmed by high-speed camera	Comparison of intrinsic infiltration rates of ethanol and water	Immersion of a defined plate into a liquid with known surface tension	Measures the diffusive reflection of defined wavenumbers
Results	contact angles	contact angles	contact angles	Potential Wettability index
Material	intact soil cores	intact soil cores	sieved soil	intact soil cores
Spatial Resolution	>4.8 mm²	0.1 mm²	>26 mm²	0.8 mm² (macro) or 0.0018 mm² (micro)

Table 4. Correlation coefficients (*a*, *b* and *c*) as derived from ANCOVA for results derived from macro DRIFTS. Coefficients according to Eq. 4 for biopores colonized and/or created by chicory (*Cichorium intybus L.*) root (R), colonized and/or created by *Lumbricus terrestris* (EW), as well as for biopores colonized and/or created by a plant root followed by colonisation of L. terrestris (REW) for 0.45-0.55 m (T1) and 0.55-0.65m (T2). Degree of freedom (dF) for *a* and *c* dF=6 or dF=546 for *b*. R^2 = 0.38.

	R		EW		REW	
	T1	T2	T1	T2	T1	T2
a			3.284			
b	-28.441	-28.567	-28.129	-28.795	-28.645	-28.530
c	-0.114	-0.142	-0.196	-0.115	-0.102	-0.119

Table 5. Means and standard deviation for contact angles derived from sorptivity tests for biopores colonized and/or created by chicory (*Cichorium intybus L.*) root (R), colonized and/or created by *Lumbricus terrestris* (EW), as well as for biopores colonized and/or created by a plant root followed by colonisation of L. terrestris (REW).

| | Contact angle [°] | | | |
	-1 kPa	-3 kPa	-6 kPa	-30 kPa
R	48.8 ± 17.1	65.7 ± 14.3	69.4 ± 8.6	56.0 ± 27.7
EW	67.0 ± 16.3	56.3 ± 16.7	75.2 ± 4.6	66.8 ± 13.6
REW	70.0 ± 4.1	72.3 ± 7.7	65.3 ± 12.9	73.0 ± 4.8
Soil matrix	46.9 ± 29.1	65.3 ± 14.4	66.0 ± 10.9	70.3 ± 6.4

Fig. 1: Sample preparation and exemplary transect (yellow, dotted line). Samples were cut off vertically, air-dried and stored in a desiccator overnight, before Diffuse Reflectance Infrared Fourier Transform Spectroscopy (DRIFTS) was performed along the transects. Results of measurements at the biopores' surface were pooled (=0 mm distance to biopore surface, **Fig. 3** and **Fig. 4**). The same was done for equidistant measurement points.
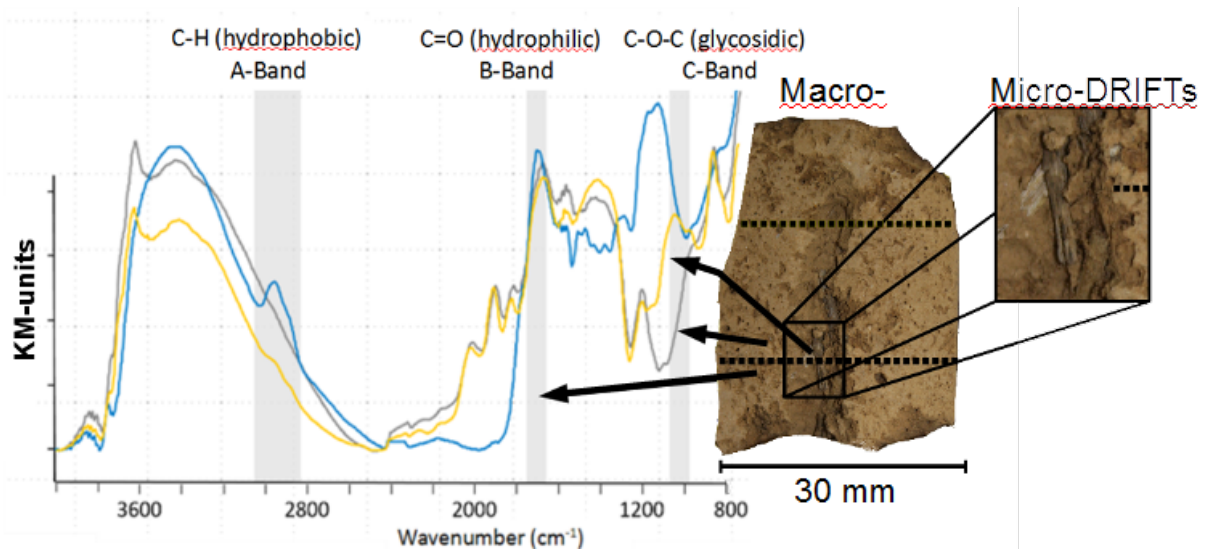
Fig. 2: Exemplary spectra as derived from macro diffuse reflectance infrared Fourier transform (macro DRIFT) spectroscopy for particulate organic matter (POM (i.e., straw residues; blue line), for soil matrix close to biopore surface (yellow line) as well as for the soil matrix more distant (grey line) to biopore surface. The right-hand side shows transects at biopore samples studied by macro- and micro-DRIFT spectroscopy.
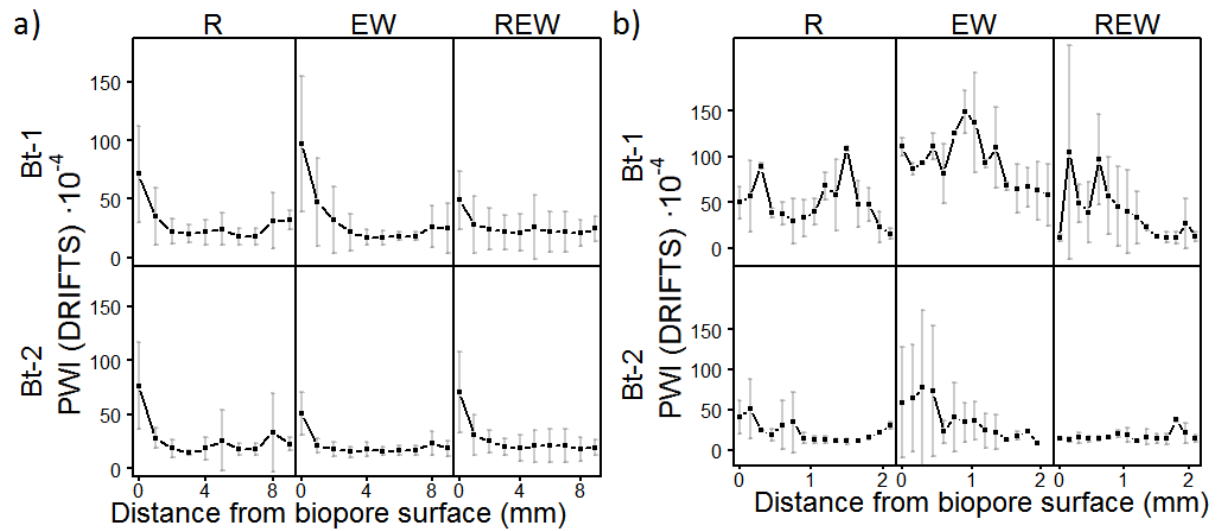
Fig. 3: Means and standard deviation for potential wettability index (PWI), derived from a) macro and b) micro diffuse reflectance infrared Fourier transform (DRIFT) spectra of biopores colonized and/or created by *Lumbricus terrestris* (EW), colonized and/or created by chicory (*Cichorium intybus L.*) roots (R), and biopores colonized and/or created by a plant root followed by colonisation of *L. terrestris* (REW). The upper row shows data for Bt-1 (0.45-0.55 m) while the lower row those for Bt-2 (0.55-0.65 m). PWI is defined as the ratio of the intensities of summed C-H signals to summed C=O signals. Results of measurements at the biopores' surface were pooled (=0 mm distance from biopore surface). The same was done for equidistant measurement points. For a) $n_{R,Bt-1}$ = 29,8,8,8,8,8,7,7,5,3; $n_{EW,Bt-1}$ = 37,8,8,8,8,8,8,8,6,4; $n_{REW,Bt-1}$ = 34,8,8,8,8,8,8,8,5,3; $n_{R,Bt-2}$ = 28,8,8,8,8,8,7,7,4,3; $n_{EW,Bt-2}$ = 33,8,8,8,8,8,8,8,5,6; $n_{REW,Bt-2}$ = 35,8,8,8,8,8,8,8,4,8. For b) n=4.
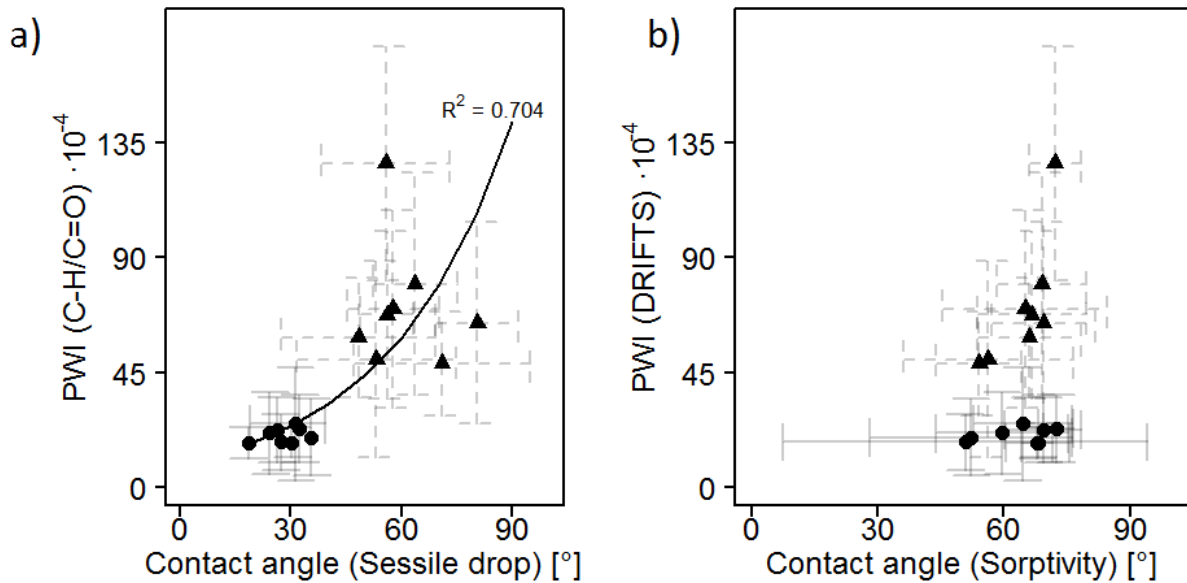
Fig. 4: Means and standard deviation of Potential wettability index (PWI) derived from macro diffuse reflectance infrared Fourier transform spectroscopy (Y-axis) plotted against contact angles derived from a) optical measurements (sessile drop) of bulk soil (distance from biopore surface ≥ 5 mm, dots) and biopore surface (triangles) or b) sorptivity tests. The biopores' histories were pooled. Results of measurements at the biopores' surface were pooled (=0 mm distance from biopore surface). The same was done for equidistant measurement points. Shown sorptivity data are for Ψ_m = -30 kPa, determined at a hydraulic gradient of +2 cm with an infiltrometer device, 0.22 mm in diameter. $n_{sorptivity}$ = 3.
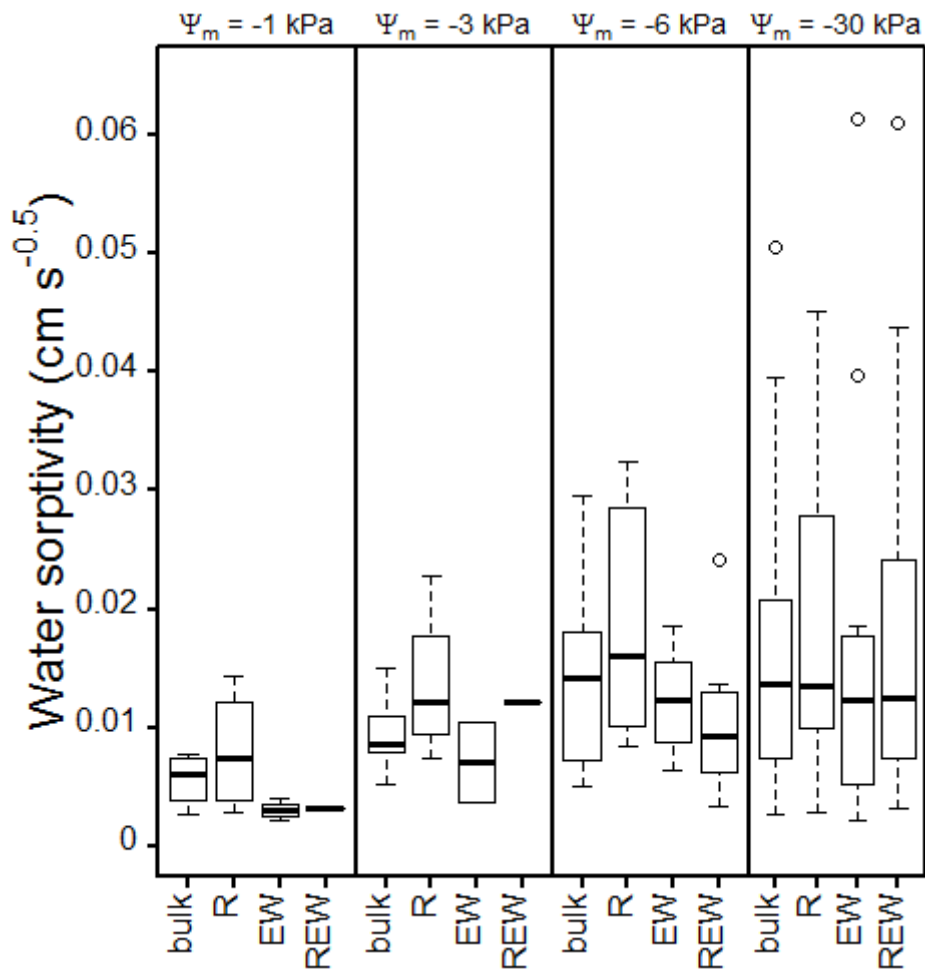
Fig. 5: Influence of matric potential and zone (bulk soil or biopore with defined history (colonized and/or created by Lumbricus terrestris (EW), colonized and/or created by chicory (Cichorium intybus L.) root (R), as well as for biopores colonized and/or created by a plant root followed by colonisation of L. terrestris (REW)) on water sorptivity. $n_{sorptivity} = 3$.
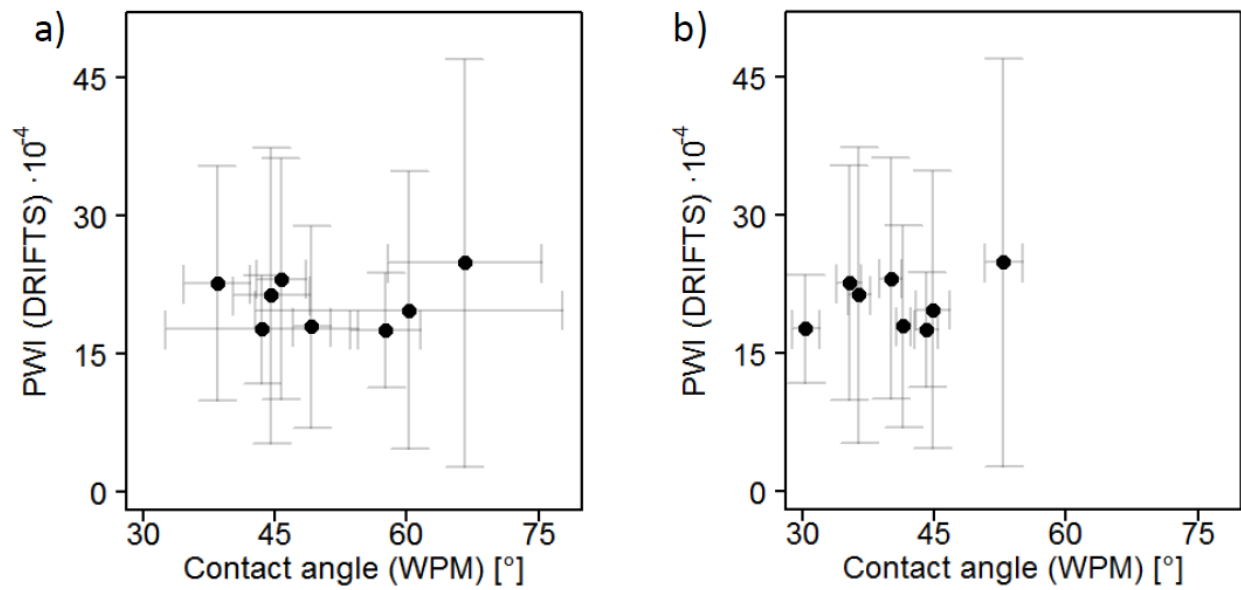
Fig. 6: Means and standard deviation for potential wettability index (PWI) as derived from macro DRIFT spectroscopy plotted against contact angles derived from Wilhelmy plate method for soil sieved to ≤ 2 mm (a) or ≤ 0.63 mm (b). Means with standard deviation for each depth and plot of the bulk soil (distance to biopore surface ≥ 5 mm). n_{WPM} = 3.